Dimensional Reduction: Synthesis and Structure of Layered $Li_5M(PO_4)_2F_2$ (M = V, Cr)

S.-C. Yin, P. Subramanya Herle, A. Higgins, N. J. Taylor, Y. Makimura, and L. F. Nazar*

Department of Chemistry, University of Waterloo, Waterloo, Ontario, Canada N2L 3G1

Received June 24, 2005. Revised Manuscript Received January 30, 2006

A new lithium vanadium fluorophosphate $Li_5V(PO_4)_2F_2$ has been synthesized by incorporation of LiF into α-$Li_3V_2(PO_4)_3$, and its structure has been determined by single-crystal X-ray diffraction. The sample crystallizes in monoclinic symmetry, space group $P2_1/c$ (No. 14), with lattice parameters $a = 6.3589(4)$, $b = 10.7795(6)$, $c = 10.3836(6)$, $\beta = 90.019(1)°$, and $Z = 4$. The refinement was performed using a total of 3094 unique reflections, resulting in agreement factors of R and wR(F^2) of 0.0422 and 0.0741, respectively. The structure of $Li_5V(PO_4)_2F_2$ consists of layers of vanadium fluorophosphate interleaved with lithium ions. Lithium ions also reside in the channels along the *a* axis and in the interstitial space within the framework. The synthesis of the title compound from α-$Li_3V_2(PO_4)_3$ represents the first example of framework reduction for a metal phosphate, from a three-dimensional to a two-dimensional structure. Bulk phases of $Li_5V(PO_4)_2F_2$ and its chromium analogue, $Li_5Cr(PO_4)_2F_2$, were also prepared from the direct reaction of MPO_4 (M = V, Cr) with LiF and Li_3PO_4. Reversible electrochemical cycling of one Li from $Li_5V(PO_4)_2F_2$ was observed at a potential of 4.15 V.

Introduction

The creation of new redox-active transition metal framework structures that host mobile interstitial lithium ions is crucial in developing potential high capacity electrodes for lithium-ion batteries. Lithium transition metal phosphates have received wide attention recently as promising positive electrodes because of their high theoretical capacity and reversibility and good electrochemical and thermal stability.[1−3] In most of the materials examined to date, these superior properties arise from a robust three-dimensional framework composed of interconnected transition metal−oxygen octahedra and phosphate tetrahedra (or "polyanions"). Lithium ions are situated in the tunnels of the framework. Typically their reversible extraction/reinsertion during electrochemical cycling results in little cell volume variation. Two phosphate structure types have been shown to have capacity superior to that of the currently commercialized layered oxide, $LiCoO_2$ (130 mA·h/g). Olivine-type $LiFePO_4$ exhibits a capacity close to theoretical (170 mA·h/g) of 150−165 mA·h/g[4,5] at relatively fast rates of charge/discharge, and a nearly theoretical capacity of 200 mA·h/g has recently been demonstrated in α-$Li_3V_2(PO_4)_3$, a NASICON-related structure.[6]

The discovery of new open-framework polyanion materials that have structural features amenable to facile lithium (de)-intercalation, along with promising redox potentials, is clearly a very desirable goal. In the search for new materials that has recently encompassed silicates and sulfates, lithium metal *fluoro*phosphates have emerged as promising candidates. These have analogues in the mineral world as hydroxyl-containing compounds where F^- partially or completely replaces an OH^- group, such as calcium hydroxyfluoroapatite. However, to be suitable as an electrode material, three characteristics are important: (1) presence of a redox center; (2) lack of electrochemically active hydroxyl groups which would undergo irreversible redox behavior; and (3) lack of structural water which could exchange into the electrolyte. Few materials have been found that meet these criteria at present. While many lithium transition metal phosphates are available synthetically or naturally as minerals, few lithium transition metal fluorophosphates are known although some sodium analogues exist. These include $Na_5Fe(PO_4)_2F_2$[7] and $Na_5Cr(PO_4)_2F_2$,[8] which have the same composition as the title compound and a similar layered framework but which crystallize in orthorhombic and trigonal symmetries, respectively. $Na_2Co(PO_4)F$ also has a layered framework structure with very unusual face sharing octahedra[9] and a layered sodium main-group compound $Na_5MF_2(PO_4)_2$ (M = Al, Ga) has been reported.[10] Other compounds such as $Na_3M_2(PO_4)_2F_3$ (M = Cr, Al, V, Fe)[11] and Na_2MnPO_4F[12] have three-dimensional frameworks; their lithium analogues have not been reported.

* To whom correspondence should be addressed. E-mail: lfnazar@uwaterloo.ca.

(1) Padhi, A. K.; Nanjudaswamy, K. S.; Goodenough, J. B. *J. Electrochem. Soc.* **1997**, *144*, 1188.
(2) Andersson, A. S.; Thomas, J. O.; Kalska, B.; Häggström, L. *Electrochem. Solid-State Lett.* **2000**, *3*, 66.
(3) Barker, J.; Saidi, M. Y. U.S. Patent 5,871,866, 1999.
(4) Ravet, N.; Goodenough, J. B.; Besner, S.; Simoneau, M.; Hovington, P.; Armand, M. *Proceedings of the 196th ECS Meeting*, Honolulu, HI, Oct. 17−22, 1999; Abstract #127 .
(5) Huang, H.; Yin, S.-C.; Nazar, L. F. *Electrochem. Solid-State Lett.* **2001**, *4*, A170.
(6) Huang, H.; Yin, S.-C.; Kerr, T.; Nazar, L. F. *Adv. Mater.* **2002**, *14*, 1525.
(7) Rastsvetaeva, R. K.; Maksimov, B. A.; Timofeeva, V. A. *Dokl. Akad. Nauk DAKNE* **1996**, *350*, 499.
(8) Nagornyi, P. G.; Kapshuk, A. A.; Kornienko, Z. I.; Mitkevich, V. V.; Tret'yak, S.-M. *Zh. Neorg. Khim.* **1990**, *35*, 839.
(9) Sanz, F.; Parada, C.; Ruiz-Valero, C. *J. Mater. Chem.* **2001**, *11*, 208.
(10) Poojary, D. M.; Clearfield, A.; Timofeeva, V. A.; Sigaryov, S. E. *Solid State Ionics* **1994**, *73*, 75. Arlt, J.; Jansen, M.; Klassen, H.; Schimmel, G.; Heymer, G. *Z. Anorg. Allg. Chem.* **1987**, *547*, 179.

10.1021/cm0513738 CCC: $33.50
Published on Web 03/04/2006

Only three lithium metal fluorophosphates have been described to date. Dutreilh et al. reported on a lithium nickel fluorophosphate, $Li_2NiF(PO_4)$, that adopts an O−F ordered anionic framework.[13] Its structure is somewhat similar to that of the title compound with respect to the arrangement of the metal−oxygen (fluorine) octahedra, although it is not isostructural. The potential for Li insertion is also predicted to be inaccessibly high, based on the voltage of the $Ni^{2+/3+}$ couple in related compounds. A cobalt analogue of this structure has also been briefly described.[14] Recently, Barker et al. reported a new lithium vanadium fluorophosphate, $LiVPO_4F$, based on the tavorite-type ($LiFePO_4OH$) structure.[15] The three-dimensional framework is composed of corner sharing V−O (F) octahedra with P−O tetrahedra. Very promising electrochemical behavior has been demonstrated for carbon composites of this material.[16]

We report here two new lithium metal fluorophosphates of the formula $Li_5M(PO_4)_2F_2$ (M = V, Cr). The vanadium fluorophosphate was first grown as single crystals from reaction of α-$Li_3V_2(PO_4)_3$ in a LiF flux, which yielded a number of needlelike prismatic crystals. While the majority had similar lattice constants, the presence of intrinsic stacking twins along the *a* axis meant that crystal fragments were used for the structure solution. We find that $Li_5M(PO_4)_2F_2$ has a novel, highly anisotropic two-dimensional structure comprised of interleaved layers of lithium ions and V−P−O(F) sheets. Furthermore, formation of this 2D structure from the reaction of the three-dimensional framework of α-$Li_3V_2(PO_4)_3$ with LiF represents an interesting example of "dimensional reduction". The concept was first outlined by Long et al.,[17] based on early observations of lowering the dimensionality of metal chalcogenides upon incorporation of highly electropositive cations or ionic salts.[18,19] The reaction we describe here represents an ideal example of this reaction in a transition metal phosphate, potentially broadening the scope of the concept and providing a route into new materials.

Following discovery of the new layered composition in single-crystal form, facile routes to prepare bulk quantities of both the V and the Cr analogues as microcrystalline powders were developed. These are also reported here.

Experimental Section

Growth of Single Crystals of $Li_5M(PO_4)_2F_2$. Single crystals of the title compound were prepared by mixing polycrystalline powders of α-$Li_3V_2(PO_4)_3$ and LiF in a 1:12 molar ratio. Microcrystalline α-$Li_3V_2(PO_4)_3$ was prepared by mixing stoichiometric amounts of Li_2CO_3 (Aldrich, 99.9%), V_2O_5 (99.6%), and $NH_4H_2PO_4$ (99.9%). The mixture was heated at 300 °C for 3 h, reground, and fired at 850 °C for 12 h under a flow of 7% H_2/N_2. The $Li_3V_2(PO_4)_3$/LiF mixture was sealed in a clean Nb tube, heated at 900 °C for 12 h, and then cooled to room temperature at 0.15 °C/min. Light green-blue crystals were selected for single-crystal X-ray structural analysis. Data sets were collected on several crystals.

Table 1. Summary of Single-Crystal Data Collection Parameters for $Li_5V(PO_4)_2F_2$

chemical formula	$Li_5V(PO_4)_2F_2$
formula weight	313.58
symmetry	monoclinic
space group	$P2_1/c$ (No. 14)
cell parameters	
a	6.3589(4)
b	10.7795(6)
c	10.3836(6)
b	90.019(1)
V	711.75(7)
Z	4
crystal description	needle prism fragment
color	light blue-green
size (mm)	0.116 × 0.100 × 0.084
calculated density (g/cm^{-3})	2.926
measuring temperature (K)	150
radiation	Mo Kα, λ = 0.710 73 Å
scan mode	*w*
θ range (deg)	$2.72 \le \theta \le 35.04$
index ranges	$-10 \le h \le 10$, $-17 \le k \le 17$, $-16 \le l \le 16$
no. measured reflections	10 013
no. independent reflections	3094
obsd reflections $I > 2\sigma(I)$	2824
no. variables	170
R(all), wR(F) (%)	4.22, 7.41
GOF	$\sigma = 1.683$
residual electron density (eÅ^{-3})	0.631, −0.540

Single-Crystal X-ray Diffraction (XRD). A 0.116 × 0.100 × 0.084 mm light green-blue crystal was mounted on a nylon fiber with perfluoropolyether oil. Data were collected at 150 K using a Bruker APEX CCD platform diffractometer with monochoromated Mo Kα (λ = 0.7107 Å) radiation. The diffraction sphere was covered by 0, 120, and 240° in φ using 0.3° steps ($2\theta_{max}$ = 70.08°) in ω. Data collection and reduction were performed with Bruker AXS SAINT and SMART5.0 program respectively, corrected for absorption by integration using the face-indexed analytical method. Transmission factors were from 0.793 to 0.867. The final unit cell parameters were determined from 6611 reflections. A total of 3094 independent reflections were used for the solution, by least-squares structural refinement (F^2) using the Bruker SHELXTL package. Final R, wR(F) and GOF were 4.22%, 7.41%, and 1.683, respectively. Detailed data collection parameters are listed in Table 1.

Preparation of Single-Phase Microcrystalline $Li_5V(PO_4)_2F_2$. *(a) $Li_5V(PO_4)_2F_2$ from $Li_3V_2(PO_4)_3$.* $Li_3V_2(PO_4)_3$ was synthesized by ball milling stoichiometric amounts of Li_2CO_3 (Alfa Aesar, 99%), NH_4VO_3 (Aldrich, 99%), $(NH_4)H_2PO_4$ (Aldrich), and ketjen black carbon. The mixture was then heated in a three-step firing process under flowing 7% H_2/N_2 gas in the following steps: 350 °C, for 5 h; then 700 °C, for 5 h; and finally, 900 °C for 6 h. The product was phase-pure (as determined by XRD) with respect to the inorganic components (although about 2% carbon was retained in the material). The resultant powder was ball milled with Li_3PO_4 (Aldrich, 99.9%) and LiF (Johnson Matthey, 99.3%) in a 1:1:4 molar ratio. This mixture was pressed into a pellet that was then placed in an alumina boat covered with Ni foam. It was fired under flowing Ar at 900 °C for 2 h.

(11) Le Mains, J.-M.; Crosnier-Lopez, M. P.; Hemon-Ribaud, A.; Courbion, G. *J. Solid State Chem.* **1999**, *148*, 260.
(12) Yakubovich, O. V.; Karimova, O. V.; Mel'nikov, O. K. *Acta Crystallogr., Sect. C* **1997**, *53*, 395.
(13) Dutreilh, M.; Chevalier, C.; El-Ghozzi, M.; Avignant, D. *J. Solid State Chem.* **1999**, *142*, 1.
(14) Okada, S.; Ueno, M.; Uebou, Y.; Yamaki J. *Proceedings of the IMLB-12*; Nara, Japan, June 27−July 2, 2004; Abstract #301.
(15) Barker, J.; Saidi, M. Y.; Swoyer, J. L. *Electrochem. Solid-State Lett.* **2003**, *6*, A1.
(16) Barker, J.; Saidi, M. Y.; Swoyer, J. L. *J. Electrochem. Soc.* **2003**, *150*, A1394. Barker, J.; Gover, R. K. B.; Saidi, M. Y.; Swoyer, J. L. *Proceedings of the IMLB-12*; Nara, Japan, June 27−July 2, 2004; Abstract #285. Barker, J.; Saidi, M. Y.; Swoyer, J. U.S. Patent 6,-387,568, **2002**.
(17) Long, J. R.; McCarty, L. S.; Holm, R. H. *J. Am. Chem. Soc.* **1996**, *118*, 4603.
(18) Kanatzidis, M. G.; Park, Y. *Chem. Mater.* **1990**, *2*, 99.
(19) Tulsky, E. G.; Long, J. R. *Chem. Mater.* **2001**, *13*, 1149.

(b) $Li_5V(PO_4)_2F_2$ from VPO_4. VPO_4 was prepared by firing a 1:1 molar ratio of NH_4VO_3 and $(NH_4)_2HPO_4$ in a flowing 7% H_2/N_2 atmosphere at 350 °C for 2 h. The powder was ball milled, returned to the furnace, and fired under the same atmosphere at 950 °C for 4 h. The product was phase-pure, as determined by XRD.

To synthesize $Li_5V(PO_4)_2F_2$, the VPO_4 was mixed with Li_3PO_4 and LiF, using a stoichiometric excess of LiF to act as a flux, thus enhancing reactivity. The reagents were ball milled together for 30 min, pressed into a pellet, and fired under flowing Ar for 15 min at 800 °C in a covered alumina boat.

A $Li_5V(PO_4)_2F_2$/carbon composite could be prepared starting from VPO_4 synthesized by carbothermal reduction from the reaction of NH_4VO_3 and $(NH_4)_2HPO_4$ (AnalaR, 99%) together in a 1:1 molar ratio along with 1.25 mol of ketjen black carbon (0.25 mol excess). These precursors were ball milled together and then fired in an alumina boat at 350 °C for 2 h under flowing N_2, ball milled again, and then refired at 950 °C for 4 h again under a flowing N_2 atmosphere. The VPO_4/C was reacted with Li_3PO_4 and LiF as above. The reagents were ball milled together and then made into a pellet. This was then fired in a covered alumina boat for 30 min at 800 °C under flowing Ar. The pellet was hand ground with a mortar and pestle for 20 min and refired under flowing Ar at 700 °C for a further 30 min. The carbon content was determined by thermogravimetric analysis to be 2−5%, as described; this content is adjustable by varying the amount of carbon initially used in preparing VPO_4.

Preparation of Single-Phase Microcrystalline $Li_5Cr(PO_4)_2F_2$. $CrPO_4$ was prepared by firing a 1:1 molar ratio of $Cr(NO_3)_3 \cdot 9H_2O$ and $NH_4H_2PO_4$ in air at 900 °C for 3 h. The product was phase-pure as determined by XRD. To synthesize $Li_5Cr(PO_4)_2F_2$, the $CrPO_4$ was mixed with Li_3PO_4 and LiF, using a stoichiometric quantity of LiF (2 molar equiv). The reagents were ground by hand, pressed into a pellet, and fired under a nitrogen atmosphere for 20 min at 850 °C in a covered alumina boat.

Electrochemical Studies of $Li_5V(PO_4)_2F_2$/C. Electrochemical evaluation of $Li_5V(PO_4)_2F_2$/C was carried out in metallic lithium test coin cells using a commercial (MacPile) multichannel galvanostat/potentiostat operating in galvanostatic mode. Typical positive electrode loadings were in the range of 5−6 mg/cm^2, and an electrode diameter of 10 mm was used throughout. The positive electrodes comprised 90 wt % active material and 10 wt % poly(vinylidene difluoride) (PVdF) binder. Carbon was not added to the electrode mixture, because conductive carbon was already incorporated in the active material $Li_5V(PO_4)_2F_2$/C composite (5% from thermal gravimetric analysis) by virtue of the synthesis method employed (see above). The electrolyte was composed of a 1 M $LiPF_6$ dissolved in ethylene carbonate (EC)/dimethyl carbonate (DMC) solution (1:1 by volume).

Results and Discussion

A. Description of the Structure. Single-crystal data sets were collected on several pale green-blue crystals of $Li_5V(PO_4)_2F_2$ as shown in Figure 1a,b. Light brown-blue crystals were also obtained in the single-crystal growth process. The light brown and green-blue crystals had almost identical lattice parameters, but satisfactory structural refinements were only obtained from the latter. On the basis of several unsuccessful refinements of the former, they represent intrinsic stacked twins resulting from mixed Li/V occupancy. The twinned portion represents a 5−10% dislocation of the entire structure by *a*/2. The twinning along the *a* axis was undoubtedly due to the layered nature of the material. A satisfactory solution was obtained from an untwinned green-blue crystal fragment.

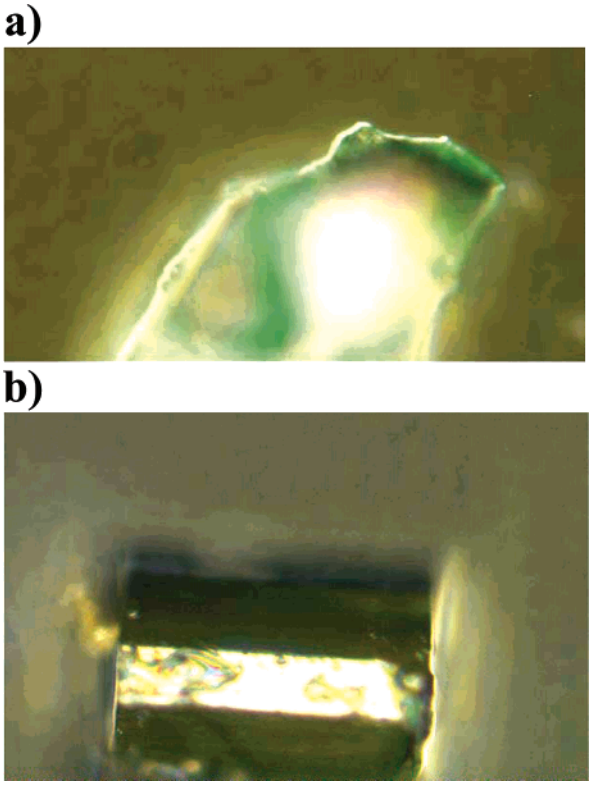

Figure 1. Images of $Li_5V(PO_4)_2F_2$ crystals viewed under a polarized microscope: (a) light blue-green phase; (b) light brown phase.

The crystal structure of $Li_5V(PO_4)_2F_2$ is depicted in Figure 2a along the *a* axis and along the *c* axis in Figure 2b. It crystallizes in monoclinic $P2_1/c$ symmetry (space group No. 14) with $\beta = 90.019°$ and lattice parameters of $a = 6.3589(4)$ Å, $b = 10.7795(6)$ Å, and $c = 10.3836(6)$Å. Attempts to refine the cell in orthorhombic *Pmma*, $Pmc2_1$, or *Pma*2 symmetries resulted in an unsatisfactory solution. The V−O (F) octahedra are isolated from each other but interconnected with corner-sharing P−O tetrahedra along the [010] and [001] directions. Two-dimensional sheets of $VO_4F_2-PO_4$, which sandwich two-dimensional layers of lithium ions that lie at $a = 1/2$, are thus contained in the (100) plane. The structure is significantly different from that of $Li_2Ni(PO_4)F$,[13] which comprises edge-shared sheets of Ni−O (F) octahedra running along the *b* axis, although connectivity in the latter (010) plane resembles that in the (100) plane of $Li_5V(PO_4)_2F_2$. The $VO_4F_2-PO_4$ framework is illustrated in Figure 3, depicting the channels that run along the *a* axis.

It is noteworthy that this framework represents an analogue of two previously reported sodium fluorophosphates, $Na_5Fe(PO_4)_2F_2$[7] and $Na_5Cr(PO_4)_2F_2$,[8] that can be prepared by direct reaction. Both structures possess two-dimensional layered transition metal fluorophosphate frameworks interleaved with layers of sodium ions that are almost identical to the lithium compound, although they crystallize in a slightly different symmetry. The former crystallizes in orthorhombic *Pbca* space group, and the latter crystallizes in the hexagonal *P*3 space group. In both structures, metal fluoro-oxygen octahedra are corner linked by phosphorus tetrahedra to form covalent sheets.

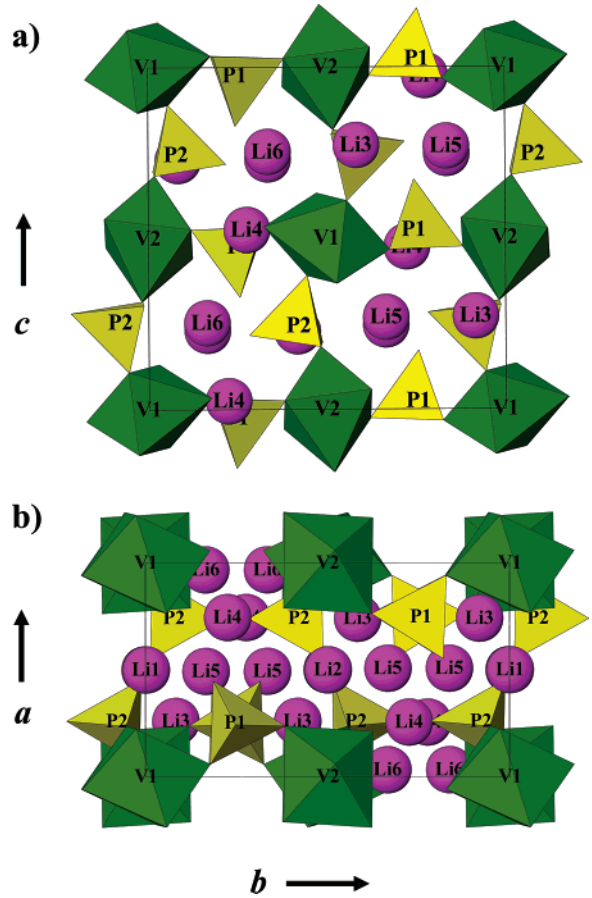

Figure 2. Structure of $Li_5V(PO_4)_2F_2$ viewed along (a) the *a* axis and (b) the *c* axis. V−O (F) octahedra, P−O tetrahedra, and lithium ions are labeled individually. V−O (F) octahedra and P−O tetrahedra are shown in green and yellow, respectively, with lithium ions shown in purple.

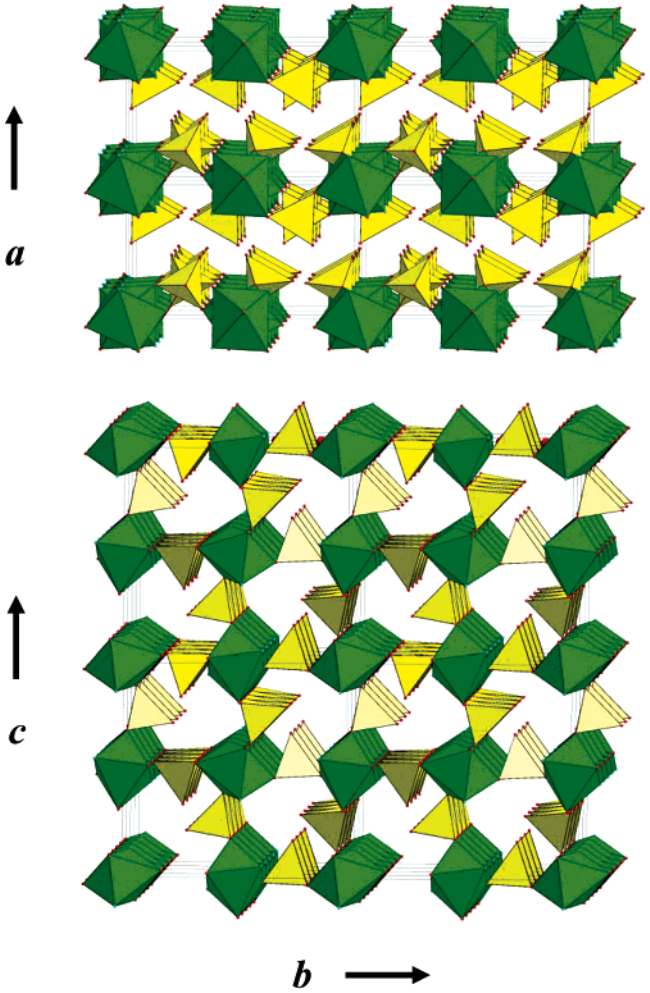

Figure 3. Depiction of the framework of $Li_5V(PO_4)_2F_2$, showing the tunnels running along the *a* axis.

B. Bonding within the $Li_5V(PO_4)_2F_2$ Framework. All vanadium [V(1), V(2)] atoms are located in the special positions (2a, 2c) of the inversion centers and are, therefore, interconnected with two distinct oxygen and one fluorine atom. Figure 4a shows the bonding environment for two vanadium atoms. Both vanadium atoms are surrounded by two fluorine atoms situated opposite to each other. An O−F ordering is also seen in the structure as in $Li_2Ni(PO_4)F$. Vanadium−oxygen bond distances range from 1.95 Å to 2.00 Å which is comparable to that in $Na_3V_2(PO_4)_2F_3$ (1.97 Å to 2.01 Å). The V(1)−F(1) and V(2)−F(2) bond lengths are 2.00 Å and 1.98 Å, respectively, which are slightly longer on average than those in $Na_3V_2(PO_4)_2F_3$ (1.88 Å and 2.02 Å).[11] The average V−O (F) distance is 1.98 Å for both V(1) and V(2) octahedra. The fluorine substitution results in slightly shorter average bond distances in the V octahedra compared to that in α-$Li_3V_2(PO_4)_3$ (2.00 Å). P(1, 2)−O tetrahedra of the title compound have little distortion with an average bond distance of 1.54 Å.

The lithium coordination environments are illustrated in Figure 4b, showing the Li−O and Li−F bonding. All lithium environments represent distorted octahedra except Li(3) and Li(5) which are five coordinate polyhedra. There are six unique lithium sites in this lithium rich phase. The "lithium layer" that lies at $a = 1/2$ contains three lithium sites: Li-(1), Li(2), and Li(5). Li(1) and Li(2) are situated within this layer at special positions (2b, 2d; inversion centers) which lie directly below vanadium atoms along the *a* axis. Li(5) is situated between Li(1) and Li(2) atoms and is located directly below Li(6), which occupies the channel along the *a* axis. The remaining interstitial space between the lithium layer and the framework is occupied by Li(3) and Li(4).

Bonding of Li−O(F) in the lithium layer is not particularly unusual. Li(1) or Li(2) possess only one distinct fluorine atom in their coordination environments. Both Li(1)−F(1) and Li(2)−F(2) bonds are long, with distances of 2.25 Å and 2.34 Å, respectively. The Li(1)−O(3, 6) and Li(2)−O(1, 5) bond lengths are normal, with distances ranging from 2.04 Å to 2.13 Å. The five coordinate Li(5) site has one particularly long Li(5)−F(1) bond at 2.54 Å, with other Li(5)−O bond distances being regular and ranging from 2.02 Å to 2.12 Å.

Li−O(F) bonding in the other sites is slightly more distorted. The five-coordinate Li(3) site possesses one particularly short Li−F bond at 1.98 Å and two average Li−O bonds: the Li(3)−O(4, 5) bond lengths are 2.02 Å and 2.00 Å, respectively. The other two Li−O bonds, Li-(3)−O(1, 8), are slightly long (2.15 Å and 2.20 Å, respectively). The Li(4)−O(F) coordination environment is similar to that in Li(1) and Li(2) where fluorine atoms lie trans to each other in the octahedra, but it is highly distorted. The Li(4)−F(2) bond distance is very short (1.88 Å) in contrast

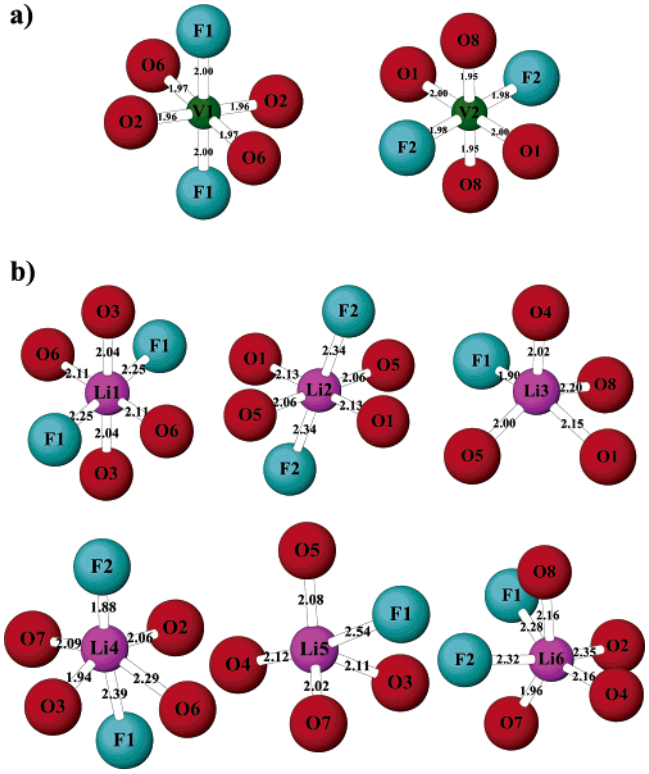

Figure 4. Vanadium (a) and lithium (b) environments in $Li_5V(PO_4)_2F_2$.

to the long Li(4)−F(1) bond (2.39 Å). The same is true of Li−O bonding, where the Li(4)−O(3, 6) bond lengths lie at 1.94 Å and 2.29 Å, respectively. The Li(6) environment is also somewhat distorted. The Li(6)−O(F) octahedra contain long adjacent Li−F(1, 2) bonds, with distances of 2.28 Å and 2.32 Å, respectively. The Li(6)−O distances are regular, except for a long Li(6)−O(2) bond of 2.35 Å.

Overall, Li−O bond distances are seen to vary from 1.94 Å to 2.35 Å which are typical of those seen in lithium metal phosphates. Li−F bond distances vary from 1.88 Å to 2.54 Å in which the majority are longer than the Li−F bond distances in ionic LiF (2.01 Å). Detailed atomic coordinates and thermal parameters are listed in Table 2, and interatomic distances are listed in Table 3.

To further differentiate energetics among the various lithium sites, bond sum calculations were performed and their values are listed in Table 4.[20] Previous studies of monoclinic $Li_3V_2(PO_4)_3$ have shown that bond sum values are a good indicator of ease-of-extraction of the lithium ion from the lattice.[21] Li(4) and Li(3) have the highest values and thus are expected to be relatively difficult to extract from the structure. In contrast, Li(6) has a relatively low bond sum and is situated in the lithium channels along the *a* axis. However, Li(5) has the lowest bond sum value and should be the most mobile as it is least tightly bound. In addition, the ion is situated in an ideal three-dimensional path for migration; namely, in the intersection of the Li channel along the *a* axis and the lithium layers, and is exchangeable with Li(6). Within the lithium layers, Li(2) is expected to be more mobile than Li(1).

C. Dimensional Reduction. Dimensional reduction is a process where an ionic component is introduced into a covalent structure, decreasing the connectivity as well as the dimensionality.[17,19] Many examples have been seen in metal chalcogenides.[18] This concept was first outlined by Long et al., based on early observations of lowering the dimensionality of metal chalcogenides by incorporation of highly electropositive cations. The idea can be applied to a binary "parent" compound MX_x that reacts with *n* moles of an ionic agent nA_aX to form a ternary "child" compound $A_{na}MX_{x+n}$, where A is typically an alkali or alkaline group element, M is a metal, and X is a chalcogenide or halide: conceptually, it was described as a "practical formalism for manipulating solid-state structures".[19] It involves deconstructing the bonding within a covalent metal−anion framework by reaction with an ionic reagent, to provide a less tightly connected framework that retains the metal coordination geometry and polyhedron connectivity of the parent structure.

By a similar concept, the reaction of ionic LiF with the three-dimensional covalent framework of α-$Li_3V_2(PO_4)_3$ yields a layered framework of $Li_5V(PO_4)_2F_2$. It represents the first example of dimensional reduction in phosphates, although the polyhedron connectivity of the parent compound is partially dismantled in this case. The process by which α-$Li_3V_2(PO_4)_3$ can be transformed to $Li_5V(PO_4)_2F_2$ is illustrated in Figure 5. Linkages between V−O octahedra and P−O tetrahedra indicated by circles are separated upon incorporation of 2 mol of LiF. Subsequent rearrangements result in formation of layers of the vanadium fluorophosphate framework, interleaved with the lithium layers.

The reaction can be described as

$$Li_3V_2(PO_4)_3 + 2LiF \rightarrow Li_5V(PO_4)_2F_2 + VPO_4 \qquad (1)$$

It is interesting to note that $LiVPO_4F$ is also prepared by incorporation of LiF into the framework of VPO_4,[15] which represents a decrease in crystal symmetry, but here, a three-dimensional framework is maintained, that is,

$$VPO_4 + LiF \rightarrow LiV(PO_4)F \qquad (2)$$

In summary, lowering the dimensionality of a metal phosphate by incorporating an alkali halide may be a useful method to prepare new structures capable of lithium intercalation.

The isolation of the title phase also suggested that the compound could be prepared directly by direct reaction of suitable precursors. This is described in the following sections for the vanadium and chromium analogues of $Li_5M(PO_4)_2F_2$ (M = V, Cr)

D. Synthesis of $Li_5V(PO_4)_2F_2$ as a Single-Phase Microcrystalline Powder. Several methods can be envisaged to form $Li_5V(PO_4)_2F_2$ by a stoichiometric route directly from starting materials, which does not leave undesirable side products such as VPO_4 (see above). The two routes we

(20) Brown, I. D. *Chem. Soc. Rev.* **1978**, *7*, 359.
(21) Yin, S. C.; Strobel, P.; Anne, M.; Nazar, L. F. *J. Am. Chem. Soc.* **2003**, *125*; 10402. Yin, S. C.; Grondey, H.; Strobel P.; Nazar, L. F. *J. Am. Chem. Soc.* **2003**, *125*, 326.

Table 2. Atomic Coordinates and Thermal Parameters of $Li_5V(PO_4)_2F_2$ (from Single-Crystal Data)

name	*x*	*y*	*z*	*U*(aniso)	fraction	site
V1	0.0000	0.0000	0.0000	0.00504(9)	0.5	2a
V2	0.0000	0.5000	0.0000	0.00504(9)	0.5	2c
P1	0.25228(7)	0.24486(4)	−0.02391(5)	0.00549(9)	1.0	4e
O1	0.23725(19)	0.38069(11)	0.02574(12)	0.0062(2)	1.0	4e
O2	0.05840(19)	0.17578(11)	0.03365(12)	0.0072(2)	1.0	4e
O3	0.44757(19)	0.18415(11)	0.03134(12)	0.0075(2)	1.0	4e
O4	0.2437(2)	0.24439(11)	−0.17161(12)	0.0084(2)	1.0	4e
P2	0.74141(7)	0.42066(4)	0.24432(4)	0.00517(9)	1.0	4e
O5	0.5459(2)	0.48654(11)	0.19560(13)	0.0077(2)	1.0	4e
O6	0.76408(19)	0.44413(11)	0.39077(12)	0.0070(2)	1.0	4e
O7	0.7395(2)	0.28209(11)	0.21687(12)	0.0080(2)	1.0	4e
O8	0.93987(19)	0.48174(11)	0.18299(12)	0.0069(2)	1.0	4e
F1	−0.22356(16)	0.02856(9)	0.13221(10)	0.0089(2)	1.0	4e
F2	−0.21151(17)	0.37695(9)	−0.05764(11)	0.0110(2)	1.0	4e
Li1	0.5000	0.0000	0.0000	0.0143(10)	0.5	2b
Li2	0.5000	0.5000	0.0000	0.0172(11)	0.5	2d
Li3	0.7408(5)	−0.0834(3)	0.2715(3)	0.0120(7)	1.0	4e
Li4	0.7448(5)	0.2237(3)	0.0250(3)	0.0098(6)	1.0	4e
Li5	0.4930(5)	0.1648(3)	0.2313(3)	0.0136(7)	1.0	4e
Li6	0.9677(6)	0.1643(3)	0.2528(4)	0.0195(8)	1.0	4e

	U11	U22	U33	U23	U13	U12
V1	0.00536(18)	0.00408(16)	0.00569(18)	0.00023(14)	−0.00045(14)	0.00011(13)
V2	0.00589(18)	0.00422(16)	0.00501(18)	0.00047(14)	0.00020(14)	0.00069(13)
P1	0.00537(19)	0.00431(18)	0.0068(2)	−0.00019(15)	−0.00026(15)	−0.00002(14)
O1	0.0072(5)	0.0047(5)	0.0068(6)	−0.0005(4)	−0.0007(4)	0.0002(4)
O2	0.0056(5)	0.0056(5)	0.0103(6)	−0.0001(4)	0.0009(5)	−0.0006(4)
O3	0.0066(6)	0.0066(5)	0.0092(6)	0.0003(4)	−0.0011(4)	0.0012(4)
O4	0.0116(6)	0.0073(5)	0.0063(6)	−0.0009(4)	−0.0005(5)	−0.0002(4)
P2	0.00543(19)	0.00485(18)	0.0052(2)	−0.00002(15)	−0.00024(14)	−0.00020(15)
O5	0.0063(5)	0.0082(5)	0.0085(6)	0.0012(5)	−0.0004(4)	0.0004(4)
O6	0.0081(6)	0.0081(5)	0.0050(6)	−0.0010(4)	−0.0009(4)	−0.0008(4)
O7	0.0096(6)	0.0052(5)	0.0093(6)	−0.0013(4)	−0.0008(5)	−0.0001(4)
O8	0.0064(5)	0.0082(5)	0.0062(6)	0.0002(4)	0.0010(4)	−0.0009(4)
F1	0.0091(5)	0.0096(5)	0.0080(5)	0.0012(4)	0.0019(4)	0.0009(4)
F2	0.0128(5)	0.0082(5)	0.0118(6)	0.0013(4)	−0.0039(4)	−0.0034(4)
Li1	0.013(2)	0.0071(19)	0.023(3)	−0.0007(18)	0.005(2)	0.0011(17)
Li2	0.019(3)	0.021(3)	0.011(2)	0.005(2)	−0.001(2)	−0.010(2)
Li3	0.0115(16)	0.0115(15)	0.0132(17)	0.0004(12)	0.0003(13)	0.0000(12)
Li4	0.0083(14)	0.0103(14)	0.0108(16)	−0.0020(12)	−0.0006(12)	0.0004(11)
Li5	0.0162(17)	0.0116(15)	0.0130(18)	0.0007(13)	0.0013(14)	−0.0031(13)
Li6	0.022(2)	0.0119(16)	0.024(2)	−0.0008(14)	−0.0083(16)	0.0046(14)

Table 3. Interatomic Distances within $Li_5V(PO_4)_2F_2$ (from Single-Crystal Data)

V1−O2[b]	1.9622(12) (×2)	Li3−F1[j]	1.897(3)
V1−O6[c,d]	1.9745(12) (×2)	Li3−O5[c]	2.003(3)
V1−F1[b]	2.0004(10) (×2)	Li3−O4[h]	2.024(3)
V2−O8[e,f]	1.9483(12) (×2)	Li3−O1[c]	2.146(4)
V2−F2[g]	1.9814(10) (×2)	Li3−O8[k]	2.200(3)
V2−O1[g]	2.0003(12) (×2)	Li4−F2[j]	1.882(3)
P1−O1[g]	1.5163(13)	Li4−O2[j]	2.062(3)
P1−O4[a]	1.5346(14)	Li4−O6[i]	2.287(3)
P1−O1[a]	1.5552(12)	Li4−F1[j]	2.388(3)
P1−O2[a]	1.5595(12)	Li4−O3[a]	1.938(3)
P2−O5[a]	1.5181(13)	Li4−O7[a]	2.090(4)
P2−O7[a]	1.5206(13)	Li5−O5[c]	2.081(4)
P2−O6[a]	1.5483(13)	Li5−O4[l]	2.118(4)
P2−O8[a]	1.5596(12)	Li5−F1[j]	2.543(4)
Li1−O3[h]	2.0390(12) (×2)	Li5−O3[a]	2.107(4)
Li1−O6[c]	2.1143(12) (×2)	Li5−O7[a]	2.019(4)
Li1−F1[b]	2.2512(11) (×2)	Li6−O8[k]	2.159(4)
Li2−O5[f]	2.0570(13) (×2)	Li6−O4[m]	2.160(4)
Li2−O1[f]	2.1254(12) (×2)	Li6−F1[j]	2.277(4)
Li2−F2[g,j]	2.3417(11) (×2)	Li6−F2[m]	2.318(4)
		Li6−O2[j]	2.351(4)
		Li6−O7[a]	1.964(4)

[a−m] Symmetry codes: (a) *x*, *y*, *z*; (b) −*x*, −*y*, −*z*; (c) −*x* + 1, *y* − 1/2, −*z* + 1/2; (d) *x* − 1, −*y* + 1/2, *z* − 1/2; (e) *x* − 1, *y*, *z*; (f) −*x* + 1, −*y* + 1, −*z*; (g) −*x*, −*y* + 1, −*z*; (h) −*x* + 1, −*y*, −*z*; (i) *x*, −*y* + 1/2, *z* − 1/2; (j) *x* + 1, *y*, *z*; (k) −*x* + 2, *y* − 1/2, −*z* + 1/2; (l) *x*, −*y* + 1/2, *z* + 1/2; (m) *x* + 1, −*y* + 1/2, *z* + 1/2.

Table 4. Bond Sum Calculations for Li Environments in $Li_5V(PO_4)_2F_2$

Li1	0.952	Li2	0.880	Li3	0.986	Li4	1.079	Li5	0.804	Li6	0.817

employed that proved most successful are

$$Li_3V_2(PO_4)_3/C + Li_3PO_4 + 4LiF \rightarrow 2Li_5V(PO_4)_2F_2/C \quad (I)$$

$$Li_3PO_4 + VPO_4 + 2LiF \rightarrow Li_5V(PO_4)_2F_2 \quad (II)$$

Reaction I yielded $Li_5V(PO_4)_2F_2$; however, the product was inevitably contaminated with large amounts of Li_3PO_4 and V_2O_3 to varying degrees (ranging up to 40%) in all the experiments attempted. Reaction II was much more successful, yielding light green $Li_5V(PO_4)_2F_2$ as a majority single phase along with some LiF impurity arising from its use as a flux in excess amount. Refinement of the diffraction pattern by Rietveld in the $P2_1/c$ space group yielded good agreement factors (Rp and wRp of 10.4% and 13.8%, respectively) as shown in Figure 6. The refined unit cell parameters of a = 6.350(4) Å, b = 10.797(1) Å, c = 10.406(1) Å, β = 90.003(4)°, and V= 713.51(2) Å^3 were in close agreement with those from single-crystal analysis (a = 6.3589(4) Å, b = 10.7795(6) Å, c = 10.3836(6) Å, and β = 90.019°; see Table 1). The analysis also revealed that the impurity phases Li_3PO_4 and V_2O_3 were present at fractions of 3.5 and 2.5%, respectively; with a LiF content ranging up to 10%. The latter can be decreased to about 2−5% by using a lower amount of flux in the synthesis, although formation of V_2O_3 then becomes more apparent.

In the above reaction, VPO_4/C was also employed as a starting reagent, synthesized by carbothermal reduction from the reaction of NH_4VO_3 and $(NH_4)_2HPO_4$ in the presence of

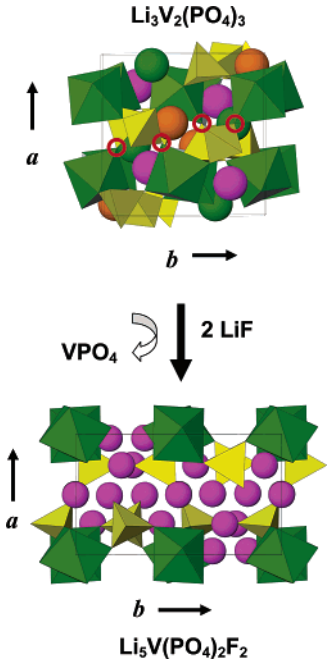

Figure 5. Illustration of the dimensional reduction process from three-dimensional α-$Li_3V_2(PO_4)_3$ to two-dimensional $Li_5V(PO_4)_2F_2$. Circles indicate separations between vanadium octahedra and phosphate tetrahedra by LiF. Rearrangements of the fluorophosphate framework yield the two-dimensional layered $Li_5V(PO_4)_2F_2$ structure.

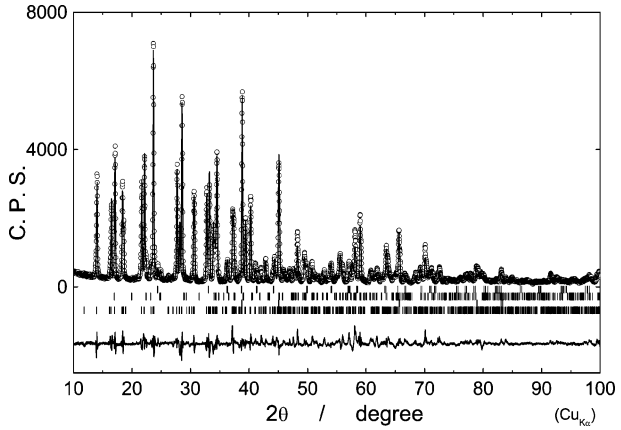

Figure 6. XRD pattern of $Li_5V(PO_4)_2F_2$ and Rietveld refinement. The experimental (○) and calculated (−) diffraction patterns are shown, along with the (*hkl*) reflections (|) and the difference curve. Lattice parameters and refinement details are as follows: $a = 6.350(4)$ Å, $b = 10.797(1)$ Å, $c = 10.406(1)$ Å, $\beta = 90.003(4)°$, and $V = 713.51(2)$ Å^3; wRp 13.8%; Rp = 10.4%.

high surface area carbon black. Carbothermal reduction is a well-known process that utilizes carbon as a reducing agent to form lower valent transition metal compounds, often in the presence of an alkali catalyst.[22] It has been recently used to prepare a variety of phosphate and fluorophosphate carbon-containing materials.[15,23] Depending on the stoichiometric ratio of carbon used in the synthesis, the VPO_4 will contain carbon in varying amounts. The carbon in the VPO_4/C precursor is carried over into the final $Li_5V(PO_4)_2F_2$ phase, to yield an intimately divided composite of the phosphate with carbon. This is advantageous to increase the electronic conductivity of the material for electrochemical studies. Optimum composite materials $Li_5V(PO_4)_2F_2$/C for this purpose were prepared with a carbon content of about 5%.

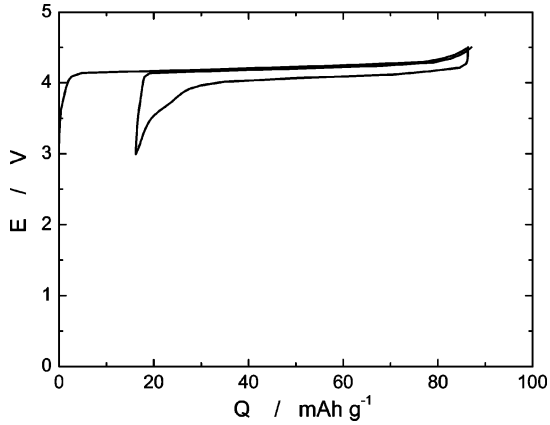

Figure 7. Electrochemical charge−discharge curve for $Li_5V(PO_4)_2F_2$/C, recorded on a cell constructed from a positive electrode containing 90% active material and 10% PVdF binder, at a current density of 0.38 mA/cm^2 (corresponding to a *C* rate of *C*/10).

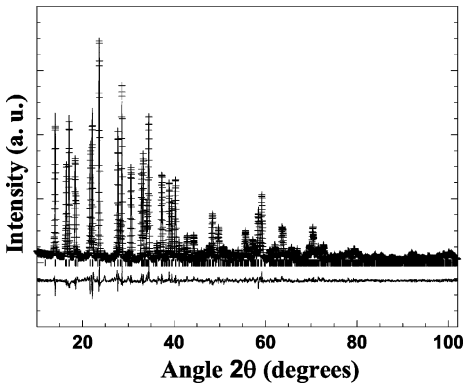

Figure 8. XRD pattern of $Li_5Cr(PO_4)_2F_2$ and Rietveld refinement. The experimental (+) and calculated (−) diffraction patterns are shown, along with the (*hkl*) reflections (|) and the difference curve. Agreement factors were the following: wRp 10.18%; $R_F^2 = 5.38$; and $\chi^2 = 4.056$. Lattice parameters and atomic coordinates are listed in Table 5.

E. Electrochemistry of $Li_5V(PO_4)_2F_2$/C. The lithium extraction/insertion behavior of $Li_5V(PO_4)_2F_2$ can, in principle, span the entire range of the $V^{3+}/V^{4+}/V^{5+}$ redox couple, $Li_5V^{III}(PO_4)_2F_2 \leftrightarrow Li_3V^{V}(PO_4)_2F_2 + 2Li^+ + 2e^-$, to give a theoretical capacity of 170 mA·h/g. On the basis of its layered framework, high accessibility of the Li^+ ions within the structure, and consideration of the stability of the oxidation states $V^{3+}-V^{4+}-V^{5+}$, we expected the material to display promising electrochemical behavior. Figure 7 shows the preliminary charge−discharge−charge behavior for a representative Li//$Li_5V(PO_4)_2F_2$/C cell. The data were acquired at constant current at an intermediate current density corresponding to C/10 (extraction/insertion of 1.0 Li in 10 h). The specific capacity of 88 mA·h/g is about half that of theoretical for extraction of two Li but very close to the full theoretical material utilization of 85 mA·h/g for one Li. There is very low voltage polarization, which is highly desirable and indicates good kinetics. The end of the charge process represents formation of a partially delithiated $Li_4V^{IV}(PO_4)_2F_2$ phase, consistent with the average voltage of 4.15 V for this process. For comparison, we note that the $V^{3+/4+}$ couple lies at about 4.2 V in $LiVPO_4F$ and at 4.1 V in $Li_3V_2(PO_4)_3$,

(22) Brauer, G., Ed. *Handbook of Preparative Inorganic Chemistry*; Academic Press: New York, 1963.
(23) Barker, J.; Saidi, Y. M.; Swoyer, J. L. *Electrochem. Solid-State Lett.* **2003**, *6*, A53.

Table 5. Atomic Coordinates and Thermal Parameters of $Li_5Cr(PO_4)_2F_2$ (Rietveld Refinement)[a]

cell parameters

space group $P2_1/c$
$a = 6.3135(2)$ Å; $b = 10.7731(2)$ Å; $c = 10.4050(2)$ Å; $\beta = 89.914(3)°$
$V = 707.71(3)$ Å^3; $Z = 4$

atomic positions

name	x	y	z	$U \times 100$	fract	site
Cr1	0.0000	0.0000	0.0000	0.68(13)	1	2a
Cr2	0.0000	0.5000	0.0000	0.92(14)	1	2c
P1	0.2486(9)	0.2465(5)	−0.0246(4)	0.55	1	4e
O1	0.2511(21)	0.3766(8)	0.0254(9)	0.62	1	4e
O2	0.0599(16)	0.1791(8)	0.0334(10)	0.72	1	4e
O3	0.4592(18)	0.1831(7)	0.0354(10)	0.75	1	4e
O4	0.2606(20)	0.2409(9)	−0.1799(8)	0.84	1	4e
P2	0.7394(10)	0.4199(4)	0.2447(5)	0.52	1	4e
O5	0.5390(18)	0.4888(14)	0.1948(8)	0.77	1	4e
O6	0.7467(24)	0.4447(7)	0.3858(8)	0.70	1	4e
O7	0.7472(19)	0.2758(8)	0.2201(9)	0.80	1	4e
O8	0.9375(16)	0.4783(11)	0.1846(8)	0.69	1	4e
F1	−0.2276(17)	0.0258(6)	0.1280(7)	0.89	1	4e
F2	−0.2134(15)	0.3781(7)	−0.0566(6)	1.10	1	4e
Li1	0.5000	0.0000	0.0000	1.43	1	4e
Li2	0.5000	0.5000	0.0000	1.72	1	4e
Li3	0.728(5)	−0.0913(24)	0.2609(29)	1.20	1	4e
Li4	0.724(6)	0.2246(23)	0.0254(25)	0.98	1	4e
Li5	0.521(6)	0.1700(23)	0.2234(49)	1.36	1	4e
Li6	0.979(5)	0.1770(21)	0.2780(54)	1.95	1	4e

[a] Refinement parameters: angular range = 10−102°; number of variables = 68, $R_{wp} = 10.18\%$; $\chi^2 = 4.056$; $R_F^2 = 5.38$.

whereas the $V^{4+/5+}$ couple in the latter is at 4.6 V. Indeed, cycling $Li_5V(PO_4)_2F_2$ to higher cutoff voltages up to 5.0 V revealed the presence of a second (shorter) plateau at about 4.7 V that corresponds to the extraction of the second Li^+ ion; however, this process was not highly reversible. Close inspection of the discharge curve also indicates the presence of a small inflection in the voltage profile at about 3.75 V, which is associated with an impurity phase. Detailed electrochemical and in situ X-ray studies are underway in our laboratory to determine the nature of this lithium insertion process, along with the long-term cycling characteristics of $Li_5V(PO_4)_2F_2$. We note that some irreversibility is observed, which may be due to slight dissolution of the positive electrode material that can be in principle optimized through careful choice of electrolyte.

F. Synthesis of $Li_5Cr(PO_4)_2F_2$. The existence of the sodium chromium analogue ($Na_5Cr(PO_4)_2F_2$) of the title structure suggested that synthesis of a lithium chromium framework might be possible. This was easily prepared by reaction of $CrPO_4$ with LiF and Li_3PO_4, the former being synthesized from $Cr(NO_3)_3 \cdot 9H_2O$ and $NH_4H_2PO_4$. Because the reaction to produce $CrPO_4$ takes place in a "solution" medium owing to the use of the nitrate hydrate, a smaller crystallite size of $CrPO_4$ results, compared to VPO_4. In turn this results in a more facile reaction and, hence, shorter reaction times (<15 min). The Rietveld refinement of the XRD pattern of $Li_5Cr(PO_4)_2F_2$ is shown in Figure 8. Only trace amounts of Li_3PO_4 are present (<1%), and, hence, inclusion of this secondary phase did not improve the refinement significantly. The structure was readily refined in the monoclinic $P2_1/c$ space group using $Li_5V(PO_4)_2F_2$ as the starting model, indicating that the compounds are isostructural. The refinement converged satisfactorily with good agreement factors of $R_{wp} = 10.18\%$, $R_F^2 = 5.38$, and $\chi^2 = 4.06$. It exhibits lattice constants ($a = 6.3135(2)$Å, $b = 10.7731(2)$Å, $c = 10.4050(2)$Å, and $\beta = 89.914(3)°$) that are only slightly contracted compared to the vanadium fluorophosphate and a lower cell volume (by 4 Å^3), as a result of the smaller size of the Cr^{3+} ion (0.62 Å) compared to that of V^{3+} (0.64 Å; see Tables 1 and 5).

Conclusions

A new layered lithium vanadium fluorophosphate, $Li_5V(PO_4)_2F_2$, has been synthesized, and single crystals were grown via the reaction of α-$Li_3V_2(PO_4)_3$ and LiF. Analysis of the single-crystal structure shows that V−O(F) octahedra and P−O tetrahedra are connected to form two-dimensional sheets. These are separated by layers of interleaved Li ions that intersect with tunnels within the framework, which are also occupied by lithium ions. Six distinct lithium sites exist within this framework. Bond sum calculations show that Li(5), which is located in the intersection of the Li tunnels along the *a* axis and the Li layers, is expected to be the most mobile ion, with the Li(6) site that possesses the next lowest bond sum also being relatively mobile. The reaction to form the title compound is analogous to the dimensional reduction reaction of metal chalcogenides by alkali halides. The material and its isostructural Cr analogue, $Li_5Cr(PO_4)_2F_2$, were also prepared as microcrystalline powders by direct reaction of precursor compounds. The cell volume of the chromium analogue is slightly lower than that of the vanadium analogue because of the smaller Cr^{3+} radius.

Both materials are capable of reversible de-intercalation of Li^+ from the structure, which in theory corresponds to the oxidation of V^{3+} to V^{5+} upon extraction of 2 mol of Li from $Li_5V(PO_4)_2F_2$ (a theoretical capacity of 170 mA·h/g) or oxidation of Cr^{3+} to Cr^{6+} upon extraction of 3 mol of Li from $Li_5Cr(PO_4)_2F_2$. The $Cr^{3+/6+}$ couple would be predicted to be at a relatively high potential, however, by comparison to the redox potential in the oxide $Li[Li_{0.2}Cr_{0.4}Mn_{0.4}]O_2$, where it lies between 2.2 and 4.5 V, at an average of 3.5 V. Typically, incorporation of phosphate groups raises the voltage as much as 1.5−2.0 V compared to the oxide, by the so-called "inductive effect".[24] Preliminary electrochemical experiments have demonstrated that lithium can be de-intercalated from $Li_5Cr(PO_4)_2F_2$ at about 4.6 V, but insertion is accompanied by a significant loss in capacity. The equilibrium potential for $Li_5V(PO_4)_2F_2$ is lower, however, and 1.0 mol of Li can be reversibly de-intercalated at an average voltage of 4.15 V, corresponding to the V^{3+}/V^{4+} couple.

AC impedance studies of ionic mobility, along with detailed electrochemical studies on these materials prepared as in situ carbon composites, are currently underway.

Acknowledgment. L.F.N. acknowledges the NSERC for funding through the Discovery and Canada Research Chair programs. S.-C.Y. thanks Dr. S. Idziak for the use of the Olympus polarizing microscope.

Supporting Information Available: Summary of the structure refinement, bond lengths, and selected angles are reported for $Li_5V(PO_4)_2F_2$ (CIF). This material is free of charge via the Internet at http://pubs.acs.org.

CM0513738

(24) Masquelier, C.; Padhi, A. K.; Nanjundaswamy, K. S.; Goodenough, J. B. *J. Solid State Chem.* **1998**, *135*, 228.